Journal of The Korean Astronomical Society
37: 477 ∼ 482, 2004

COSMIC RAYS ACCELERATED AT SHOCK WAVES IN LARGE SCALE STRUCTURE

Dongsu Ryu[1] and Hyesung Kang[2]
[1]Department of Astronomy & Space Science, Chungnam National University, Daejon 305-764, Korea
[2]Department of Earth Sciences, Pusan National University, Pusan 609-735, Korea
E-mail: ryu@canopus.chungnam.ac.kr, kang@uju.es.pusan.ac.kr

ABSTRACT

Shock waves form in the intergalactic space as an ubiquitous consequence of cosmic structure formation. Using N-body/hydrodynamic simulation data of a ΛCDM universe, we examined the properties of cosmological shock waves including their morphological distribution. Adopting a diffusive shock acceleration model, we then calculated the amount of cosmic ray energy as well as that of gas thermal energy dissipated at the shocks. Finally, the dynamical consequence of those cosmic rays on cluster properties is discussed.

Key words : cosmic rays – large scale structure of universe – shock waves

I. INTRODUCTION

Intergalactic shock waves develop as a consequence of the large scale structure formation of the universe (see, e.g., Ryu & Kang, 1998; Quilis *et al.*, 1998; Miniati *et al.*, 2000; Ryu *et al.*, 2003; Gabici & Blasi, 2003). Those cosmological shock waves, like most astrophysical shocks, are collisionless features mediated by collective, electromagnetic viscosities. Through dissipation the cosmological shock waves convert a part of the gravitational energy associated with structure formation into heat. At the same time, due to incomplete plasma thermalization at collisionless shocks, a sizable portion of the shock energy can be converted into cosmic ray (CR) energy (mostly ionic) via diffusive shock acceleration (Kang *et al.*, 1996; Miniati *et al.*, 2001b,a; Ryu *et al.*, 2003; Gabici & Blasi, 2003) (see, also Blasi, 2004; Miniati, 2004).

Diffuse synchrotron radio halos or/and radio relics have been observed in a number of clusters, indicating the existence of CR electrons as well as magnetic field in the intracluster medium (ICM) (Feretti *et al.*, 2004; Giovannini & Feretti, 2004). In addition, EUV and/or hard X-ray radiation excesses over the thermal X-ray from hot gas has been reported in some clusters, which are due to inverse-Compton scattering of cosmic background radiation photons by CR electrons (Bowyer, 2004; Henriksen & Hudson, 2004). If some of those CR electrons have been energized at cosmological shock waves, the same process should have produced a greater CR proton population, although the existence of CR protons in the ICM is yet to be confirmed by observations of γ-rays by inelastic collisions between CR and thermal-gas protons (Reimer, 2004).

In this paper, first we describe the distribution and properties of cosmological shock waves, studied in a numerical simulation of the ΛCDM cosmology. Then, we present an estimate for the amount of CR protons that should have been accelerated in those shocks. We find that the energy of the CR protons in the ICM could be a significant fraction of gas thermal energy. Finally, we describe the possible influence of such CRs on the properties of clusters/groups, again studied with numerical simulations of the ΛCDM cosmology.

II. SHOCK WAVES IN LARGE SCALE STRUCTURE

To study the distribution and properties of cosmological shock waves, the data from an N-body/hydrodynamic simulation of a ΛCDM universe with radiative cooling were used. The simulation was performed using a PM+Eulerian hydrodynamic cosmology code that was specifically designed to capture shocks with a high accuracy (Ryu *et al.*, 1993). The ΛCDM model adopted the currently favored values of the following cosmology parameters: $\Omega_{BM} = 0.043$, $\Omega_{DM} = 0.227$, $\Omega_\Lambda = 0.73$ ($\Omega_{BM} + \Omega_{DM} + \Omega_\Lambda = 1$), $h \equiv H_0/(100$ km/s/Mpc$) = 0.7$, and $\sigma_8 = 0.8$. These values are consistent with those fitted with the recent WMAP data (see, *e.g.,* Spergel *et al.*, 2003). A cubic region of size $L = 100h^{-1}$Mpc at present was simulated inside the computational box with 1024^3 grid zones for gas and gravity and with 512^3 particles for dark matter.

Shock waves, which were created by supersonic flow motion in the course of large scale structure formation, were identified in the simulation and their characteristics were quantified (see Ryu *et al.*, 2003; Kang *et al.*, 2005, for details). Based on close examination of shock locations and the properties of the shocks and their associated flows, we classified cosmological shock waves into two categories, *external* and *internal* shocks. External shocks surround sheets, filaments and knots, forming when never-shocked, low density, void gas accretes onto those nonlinear structures. Internal shocks

Proceedings of The 3rd Korean Astrophysics Workshop on *Cosmic Rays and Magnetic Fields in Large Scale Structure*

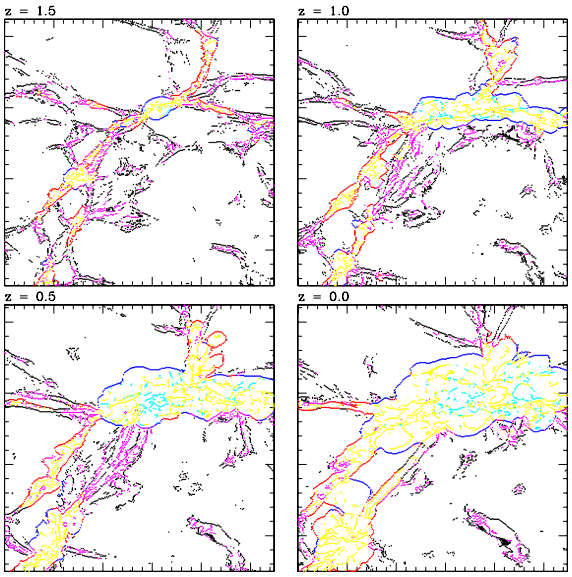

Fig. 1.— Time evolution of shock wave distribution around a cluster complex in a two-dimensional slice of $28h^{-1} \times 37h^{-1}$ Mpc^2. Color indicates shocks of different categories: black - external shocks with $v_{\rm sh} < 150$ km s^{-1}, red - external shocks with $150 < v_{\rm sh} < 700$ km s^{-1}, blue - external shocks with $v_{\rm sh} > 700$ km s^{-1}, magenta - internal shocks with $v_{\rm sh} < 150$ km s^{-1}, yellow - internal shocks with $150 < v_{\rm sh} < 700$ km s^{-1}, and cyan - internal shocks with $v_{\rm sh} > 700$ km s^{-1}.

form and are distributed within the regions bounded by external shocks. Figure 1 shows in a two dimensional slice the time evolution of shock waves identified around a cluster complex. It plots the distributions of external and internal shocks, which were coded with different colors depending on shock speed.

It is expected that the speed of cosmological shock waves reflects the depth of gravitational potential wells of nonlinear structures, and hence their morphology. In the simulation, 1) high-speed shocks with $v_{sh} \gtrsim 700$ km s^{-1} are found mostly around and inside *knot-like* structures of clusters/groups, 2) shocks with 150 km s^{-1} $\lesssim v_{sh} \lesssim$ 700 km s^{-1} mostly around and inside *filamentary* structures, and 3) low-speed shocks with $v_{sh} \lesssim 150$ km s^{-1} mostly around and inside *sheet-like* structures. Figure 2 display the volume rendering images of shock waves with three ranges of speed in small regions of computational box. The figure demonstrates clearly that the morphology of nonlinear structures can be revealed through the distributions of shocks with different speeds.

In order to quantify the occurrence of shocks, the surface area of identified shocks per logarithmic Mach number interval, $dS(M,z)/d\log M$, normalized by the volume of the simulation box, was calculated. Figure 3 shows $dS(M,z)/d\log M$ for external and internal shocks at several epochs. A few points are noticed. 1)

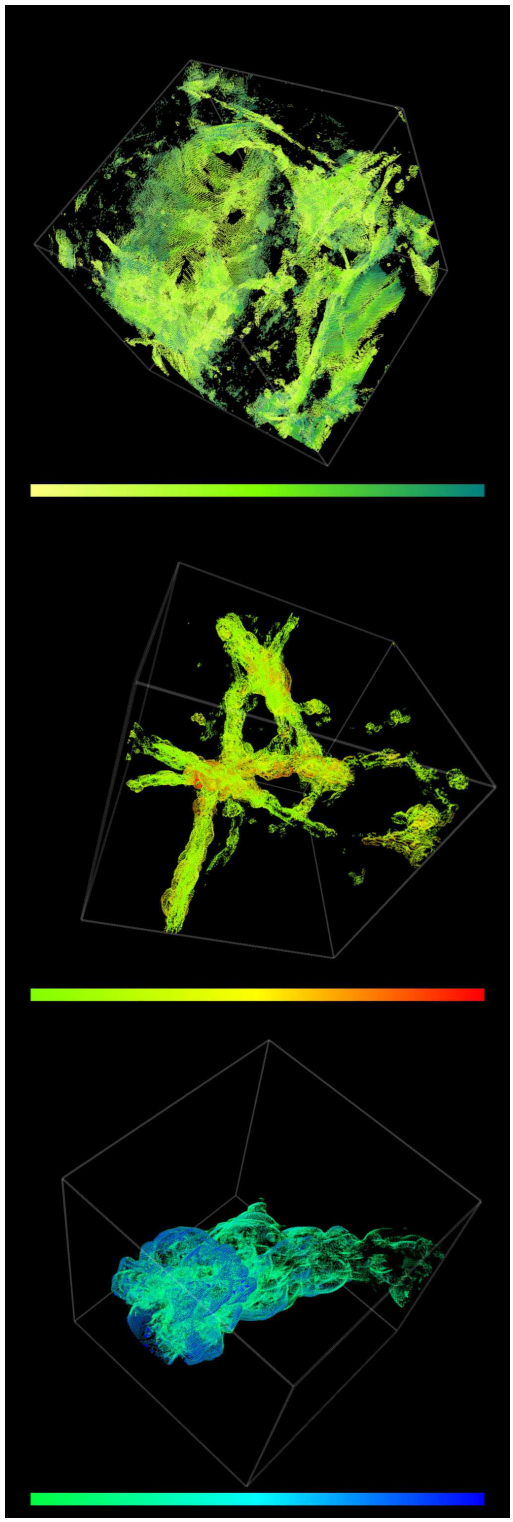

Fig. 2.— Volume rendering of three-dimensional shock wave distribution at $z = 0$. *Top panel*: shock waves with $v_{\rm sh} < 150$ km s^{-1} in a region of $(25\ h^{-1}{\rm Mpc})^3$. *Middle panel*: shock waves with $150 < v_{\rm sh} < 700$ km s^{-1} in a region of $(31\ h^{-1}{\rm Mpc})^3$. *Bottom panel*: shock waves with $v_{\rm sh} > 700$ km s^{-1} in a region of $(25\ h^{-1}{\rm Mpc})^3$.

At present, the mean distance between shock surfaces over all the computational volumes is $\sim 3h^{-1}$ Mpc. The mean distance between shock surfaces inside nonlinear structures is $\sim 1h^{-1}$ Mpc. 2) At present, external shocks are more common than internal shocks. The total surface area of external shocks is about twice of that of internal shocks. 3) External shocks are stronger with Mach number extending up to several hundreds, while internal shocks are weaker with Mach number mostly less than ~ 10. It is because the preshock gas has $T \sim 10^4$ K for external shocks, but it is much hotter for internal shocks. However, although the mean Mach number is higher for external shocks, the mean shock speed is actually larger for internal shock. In addition, the preshock gas density is significantly higher for internal shocks.

III. CRS ACCELERATED AT COSMOLOGICAL SHOCKS

To estimate the amount of CR protons accelerated at cosmological shock waves, we calculated the following energy fluxes through shock surfaces: 1) the kinetic energy flux, $f_\phi = (1/2)\rho_1 v_{\rm sh}^3$; 2) the thermal energy flux generated at shocks, $f_{\rm th}$; 3) the CR energy extracted, *i.e.,* nonthermal dissipation, at shocks, $f_{\rm CR}$. The thermal energy flux was computed from the Rankine-Hugoniot jump condition. Then, the ratio $f_{\rm th}/f_\phi \equiv \delta(M)$ can be defined as the efficiency of shock thermalization. Similarly, the efficiency of CR acceleration, $f_{\rm CR}/f_\phi \equiv \eta(M)$, can be defined as well. The efficiency $\eta(M)$ can be estimated with nonlinear numerical models of diffusive shock acceleration (DSA) at quasi-parallel shocks. We computed the values of $\eta(M)$ using one-dimensional simulations of CR proton acceleration and accompanying CR-modified flow evolution for shocks with $v_{\rm sh} = 1500 - 3000$ km s^{-1} propagating into media of $T = 10^4 - 10^8$ K, assuming Bohm-type diffusion for CRs (Kang & Jones, 2004).

The thermal and CR energies dissipated at shock surfaces can be calculated by convolving the shock Mach number distribution in Figure 3 with $\delta(M)$ and $\eta(M)$. To measure the dissipations at shocks as well as the kinetic energy flux through shocks over the cosmological time scale, we integrated those quantities from $z = 2$ to $z = 0$, $dY_i(M)/d\log M$, with $i \equiv \phi$ (for kinetic energy flux), th, and CR. We also summed these time-integrated quantities to calculate the associated global shock-processed quantities, $Y_i(> M)$. Figure 4 shows $dY_i(M)/d\log M$ and $Y_i(> M)$ for external and internal shocks. The figure indicates that energetically internal shocks are more important than external shocks, although they are less common. It is because internal shocks have higher preshock density and velocity, as noted in the previous section. Specifically, internal shocks with $2 \lesssim M \lesssim 5$ are most important, accounting for $\sim 1/2$ of CR energy generation. With the DSA model we adopted, the ratio of the CR to thermal energies dissipated at cosmological shock waves with the Mach number greater than 1.5 is $Y_{\rm CR}(\geq 1.5)/Y_{\rm th}(\geq 1.5) \approx 1/2$.

IV. DYNAMICAL INFLUENCE OF CRS ON CLUSTERS

The time scales of CR proton trapping and energy loss are larger than the Hubble time scale in most energy range. Hence, once generated, CR protons should fill the volume inside filaments and sheets as well as in clusters/groups. The existence of substantial CR protons should have affected the evolution and the dynamical status of the large scale structure of the universe.

To study the influence of such CRs, we performed an additional set of numerical simulations, where the dynamical effects of CRs were included explicitly. The simulations employed the ΛCDM cosmology same as that described in §II. But a cubic region of size $75h^{-1}$ Mpc at the current epoch was simulated inside a computational box with 512^3 gas, CR and gravity zones and 256^3 dark matter particles. Two simulations were done, one with CRs included and the other without CRs. The convection equation for the CR energy was solved explicitly in a two-fluid approximation, in addition to the standard set of equations for dark matter and gas. It was assumed that the sources (AGNs), which deposit CRs into the ICM, form at 40 different epochs after the redshift $z = 10$, if the following criteria are satisfied in each grid zone

$$M_{\rm gas} \geq \frac{4\times 10^{10}}{(1+z)^{1/5}} h^{-1} M_\odot, \quad \frac{\partial u_k}{\partial x_k} < 0, \qquad (1)$$

where $M_{\rm gas}$ is the total gas mass inside the zone and u_k is the flow velocity. It was further assumed that each source ejects the following amount of CR energy into the ICM

$$E_{\rm CR} = 3\times 10^4 h^{-1} M_\odot \times c^2. \qquad (2)$$

Note that at $z = 0$ this translates into the CR efficiency, $E_{\rm CR}/M_{\rm gas}c^2 = 7.5\times 10^{-7}$. With the above model for CR deposit, the CR energy density in the ICM becomes $\sim 1/2$ of the gas thermal energy density at $z \sim 1$ and stays constant afterwards.

The global effect of CRs on the growth of the large scale structure is exhibited in Figure 5. With $E_{\rm CR} \sim 1/2 E_{\rm th}$ on average, the power of density perturbation was decreased by $\sim 50\%$ at the present epoch on the cluster scale of $\sim 1h^{-1}$ Mpc. However, the structures of scales larger than the cluster scale have been less affected. It is because the sources formed mostly at the highest density peaks within clusters/groups, but also it is expected that the dynamical effects of CR pressure as well as thermal pressure are most important in the ICM.

In order to examine the dynamical effects of CRs on individual clusters/groups, we identified them in simulation data and calculated their properties, such as X-ray luminosity, L_x, gas mass, $M_{\rm gas}$, temperature, T_x,

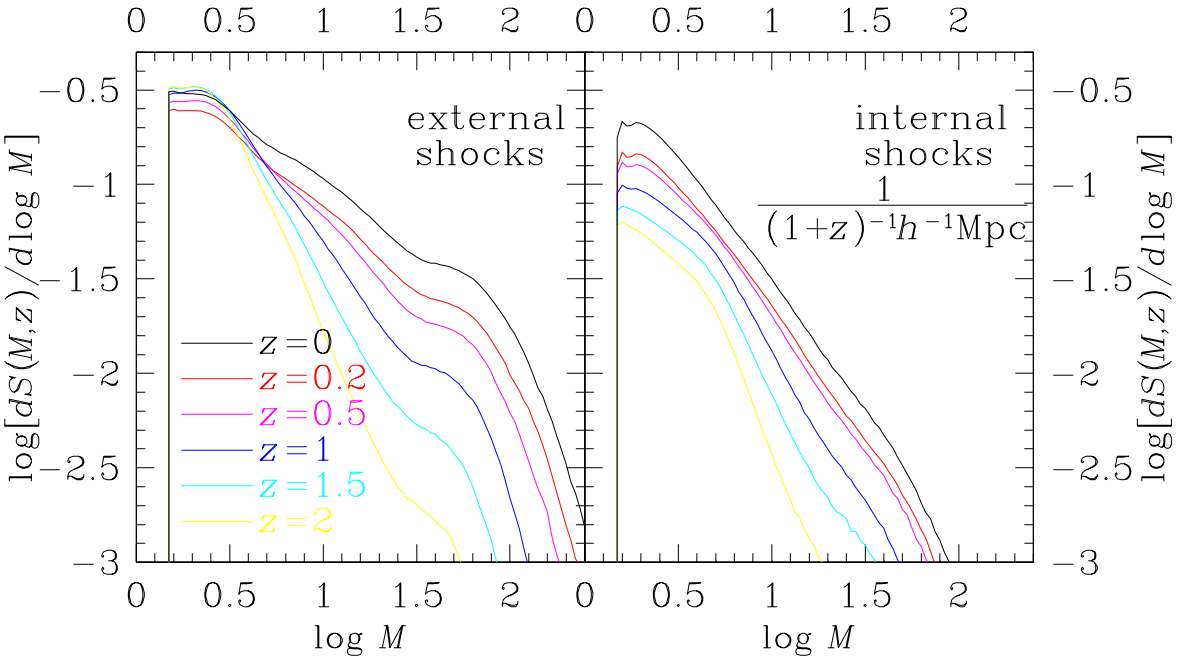

Fig. 3.— Inverse of the mean comoving distance between shock surfaces with Mach number between $\log M$ and $\log M + d(\log M)$ at different redshifts, $dS(M, z)$, for external shocks (*left panel*) and internal shocks (*right panel*).

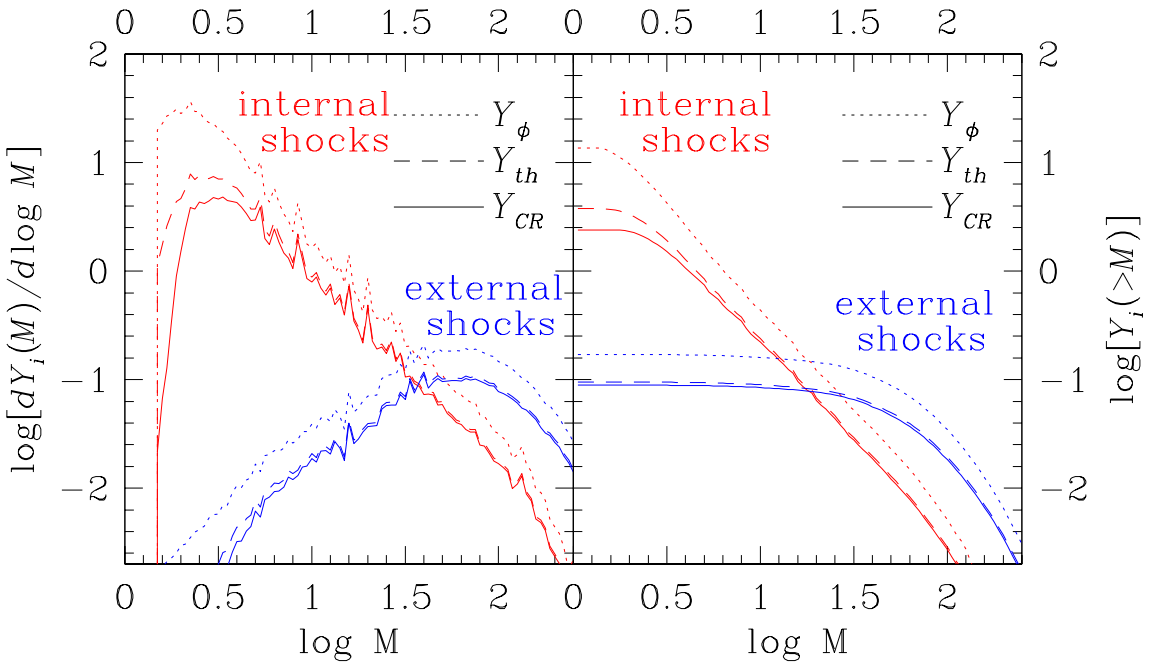

Fig. 4.— *Left panel*: kinetic energy, $dY_\phi(M)$, thermal energy, $dY_{th}(M)$, and CR energy, $dY_{CR}(M)$, processed through surfaces of external and internal shocks with Mach number between $\log M$ and $\log M + d(\log M)$, from $z = 2$ to $z = 0$. *Right panel*: same energies, $Y_\phi(> M)$, $Y_{th}(> M)$, $Y_{CR}(> M)$, processed through surfaces of external and internal shocks with Mach number greater than M, from $z = 2$ to $z = 0$. The energies are normalized to the total gas thermal energy, $\mathcal{E}_{th}$, inside simulation box at $z = 0$.

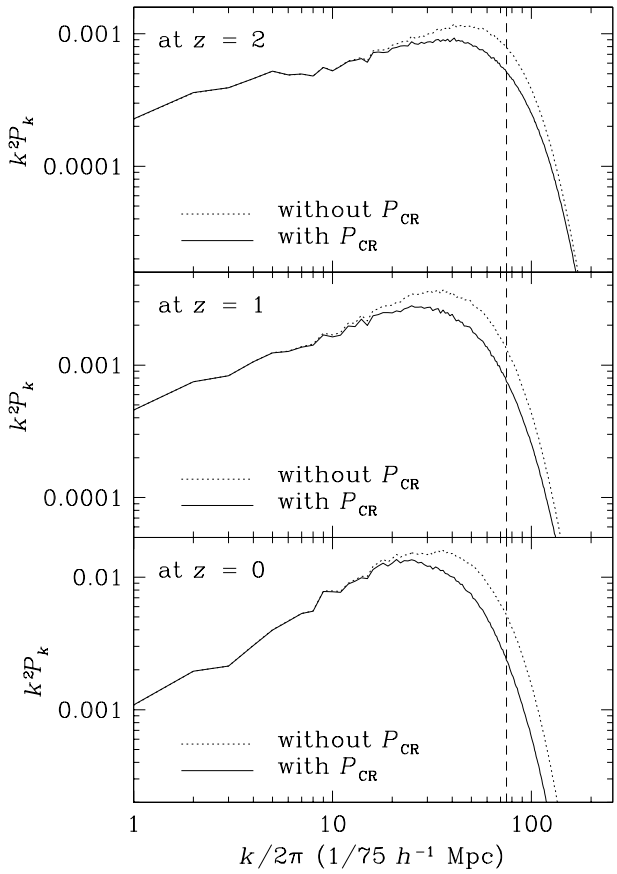

Fig. 5.— Power spectrum of gas density perturbations at three different epochs. Solid lines are from the simulation with CRs and dotted lines are from the simulation without CRs. Vertical line marks the scale of $1h^{-1}$ Mpc.

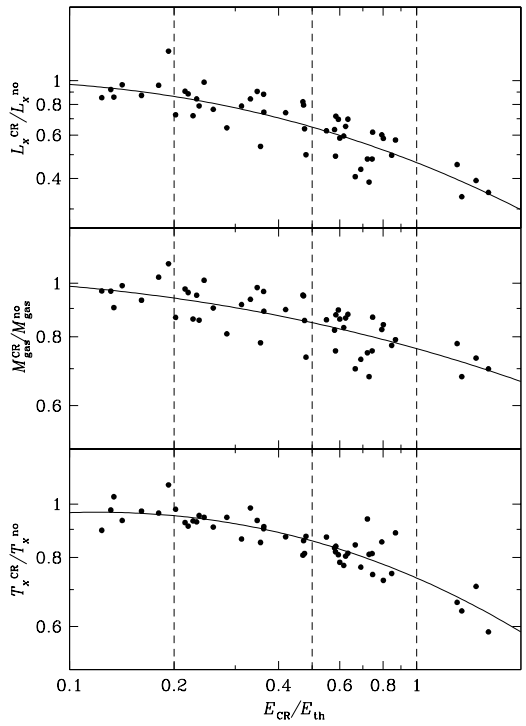

Fig. 6.— Ratios of X-ray luminosity (*top panel*), mass (*middle panel*) and temperature (*bottom panel*) for the same clusters/groups but with/without CRs, as a function of the ratio of CR to thermal energies. 50 clusters/groups are shown. Solid lines represent the least square fits. Vertical lines mark $E_{\rm CR}/E_{\rm th} = 0.2$, 0.5, and 1.

gas thermal energy, $E_{\rm th}$ and CR energy $E_{\rm CR}$. We found that the slopes of the $L_x - T_x$ and $M_{\rm gas} - T_x$ relations do not change noticeably. However, the additional CR pressure reduces L_x, $M_{\rm gas}$, and T_x of identified clusters/groups. Quantitative estimates of changes in these cluster properties can be seen in Figure 6, which shows the ratios of L_x, $M_{\rm gas}$, and T_x for the same clusters without/with CRs, as a function of $E_{\rm CR}/E_{\rm th}$. Here, $E_{\rm th}$ is the gas thermal energy of clusters with CRs. Clusters have the values of $E_{\rm CR}/E_{\rm th}$ between 0.1 to 2 due to statistical fluctuation of CR sources. In the clusters with $E_{\rm CR}/E_{\rm th} \sim 1/2$, we can see that $M_{\rm gas}$ and T_x are reduced by $\sim 15\%$ due to CRs, while L_x is reduced by $\sim 30\%$.

ACKNOWLEDGEMENTS

DR and HK acknowledge P. L. Biermann, T. W. Jones, E. Hallman for collaborations and discussions. DR was supported in part by a grant of the Chungnam National University 2004 R&D Project. HK was supported in part by KOSEF through Astrophysical Research Center for the Structure and Evolution of Cosmos (ARCSEC)

REFERENCES

Bowyer, S. 2004, in Proc. of the "International Conference on Cosmic Rays and Magnetic Fields in Large Scale Structure", eds. D. Ryu & H. Kang

Blasi, P. 2004, in Proc. of the "International Conference on Cosmic Rays and Magnetic Fields in Large Scale Structure", eds. D. Ryu & H. Kang

Feretti, L., Brunetti, G., Giovannini, G., Kassim, N., Orrú, E. & Setti, G. 2004, in Proc. of the "International Conference on Cosmic Rays and Magnetic Fields in Large Scale Structure", eds. D. Ryu & H. Kang

Gabici, S. & Blasi, P. 2003, ApJ, 583, 695

Giovannini, G. & Feretti, L. 2004, in Proc. of the "International Conference on Cosmic Rays and Magnetic Fields in Large Scale Structure", eds. D. Ryu & H. Kang

Henriksen, M. & Hudson, D. 2004, in Proc. of the "International Conference on Cosmic Rays and Magnetic Fields in Large Scale Structure", eds. D. Ryu & H. Kang

Kang, H. & Jones, T. W. 2004, in Proc. of the "International Conference on Cosmic Rays and Magnetic Fields in Large Scale Structure", eds. D. Ryu & H. Kang

Kang, H., Ryu, D., Cen, R. & Song, D. 2005, ApJ, 619, in press

Kang, H., Ryu, D. & Jones, T. W. 1996, ApJ, 456, 422

Miniati, F., Jones, T. W., Kang, H. & Ryu, D. 2001a, ApJ, 562, 233

Miniati, F., Ryu, D., Kang, H. & Jones, T. W. 2001b, ApJ, 559, 59

Miniati, F., Ryu, D., Kang, H., Jones, T. W., Cen, R. & Ostriker, J. 2000, ApJ, 542, 608

Miniati, F. 2004, in Proc. of the "International Conference on Cosmic Rays and Magnetic Fields in Large Scale Structure", eds. D. Ryu & H. Kang

Quilis, V., Ibanez, J. M. A. & Saez, D. 1998, ApJ, 502, 518

Reimer, O. 2004, in Proc. of the "International Conference on Cosmic Rays and Magnetic Fields in Large Scale Structure", eds. D. Ryu & H. Kang

Ryu, D. & Kang, H. 1998, in Proc. of the "18th Texas Symposium on Relativistic Astrophysics", (Singapore: World Scientific), eds. A. Olinto, J. Frieman & D. Schramm, p. 572

Ryu, D., Kang, H., Hallman, E. & Jones, T.W., 2003, ApJ, 593, 599

Ryu, D., Ostriker, J. P., Kang, H. & Cen, R. 1993, ApJ, 414, 1

Spergel, D. N. *et al.* 2003, ApJS, 148, 175